Master QLMN Pascal Scholl
Experimental quantum computing pascal.scholl@pasqal.com

Lecture 2 - Quantum computing using atomic qubits: Neutral atoms and ions

December 17th 2025

Atoms are natural objects to use for performing quantum computing. As seen in the previous lecture, the main requirements for performing quantum computing are (1) high quality qubits, and (2) a large quantity of qubits. Atoms match these two requirements.

First, the electrons gravitating around the nucleus possess well-defined energy levels governed by the laws of quantum mechanics. Although they intrinsically have more than two energy levels, over the last 50 years atomic physicists have developed methods to prepare, measure, and control a subset of these energy levels in order to create and manipulate qubits. Such control enabled the construction of the most precise clocks developed by humankind. These instruments are nowadays for example used to measure time (definition of the second in the International System of Units), or to measure other quantities related to time, such as precise measurement of the gravitational field.

Second, atoms of a given species are all identical. This means that all the qubits will interact in exactly the same way with their environment, a crucial feature for scaling up in qubits number while preserving high quality qubits. Further, we will see next that the commonly used species are naturally present on earth. As one gram of matter holds $\sim 10^{23}$ atoms, it means that, in principle, very few resources at the qubit level are necessary to build efficient quantum computers.

This lecture describes two currently leading platforms for performing quantum computing using atomic qubits: neutral atoms in optical tweezers, and trapped ions. These two platforms are based on the same elementary particle (the atom), and use the same elementary laws to manipulate and process quantum information (light-matter interactions and atomic physics). The aim of this lecture is to present the key working principles of these two platforms, from the qubit isolation and manipulation to the gates operations.

Atomic qubits platforms encode quantum bits into the energy levels of *electrons* gravitating around the nucleus. Among all the possible states of these electrons, two states, which we call $|0\rangle$ and $|1\rangle$, are selected as a qubit basis.

We will first detail how these platforms isolate the qubits, which will motivate the choice for specific atomic species. We will then describe how these atomic qubits can be manipulated for the aim of performing quantum computations, and the typical qubit quality that is reached, defining the choice for the best qubit encoding amongst the atomic qubit electronic levels. We will then detail how to implement the gates that were introduced in Lecture 1: single-qubit gates, and two-qubit gates. We will finally summarize the typical nowadays performances of these platforms.

1 Isolation of atomic qubits via trapping

In order to ease manipulation, atomic qubits are located at controlled positions in space. In other words, atomic qubits are *individually trapped*. As the trapping techniques strongly differ between neutral atoms and ions, we successively describe them.

1.1 Trapping neutral atoms using optical tweezers

In order to trap neutral atoms, laser cooling and trapping techniques are used. Single atoms have very little mass so an atom in equilibrium with a room temperature bath has a thermal speed $\frac{1}{2}mv^2 = \frac{3}{2}k_BT$, where v is the atom velocity, m is the atomic mass, T the temperature, and k_B the Boltzmann constant. For typically used atomic species, we obtain $v = 240\,\mathrm{m/s}$. In order to trap such high-speed atoms, the adopted solution is the following:

- The atoms are first laser cooled to μK temperatures. Laser cooling relies on photon momentum to reduce the kinetic energy of atoms. Assuming a two level system and a photon with momentum $p_\nu = \hbar k$ with $\hbar$ the reduced Planck's constant and k the photon's propagation axis, after a cycle of photon absorption and spontaneous emission, an atom with initial velocity v_i reaches a velocity v_f given by $mv_f = mv_i + \hbar(k - k_{\mathrm{sp}})$ where k_{sp} denotes the direction of the spontaneously emitted photon. Since the direction of k_{sp} is randomly distributed, in the laser beam propagation axis its impact can be neglected over many realizations. Therefore, a single laser beam will push the atoms along its propagation axis. In order to cool the atoms and reach a steady state, we apply a pair of counter-propagating beams, and set the frequency of the laser to be out of resonance from the atomic transition by a quantity $\Delta < 0$. If the atoms are propagating towards beam A, thanks to the Doppler effect, Δ increases for this beam (an decreases for beam B) and thus the beam pushes the atom in the other direction with a strength larger than beam B. The equilibrium atomic temperature depends on Δ and can be shown to be $k_BT_D = \hbar\gamma/2$ for $\Delta = -\gamma/2$, where γ is the transition linewidth. This technique is applied in the three directions of space (6 laser beams in total), and allows to reach temperature in the hundred μK range.

- Atoms are then individually trapped using laser light which is strongly focused onto the atoms (typically a volume of $1\,\mu\mathrm{m}^3$), also called *optical tweezers* due to their ability to "catch" single atoms. The laser is usually largely detuned from the atomic resonance, such that the absorption rate of the light is in the range of one photon per second (this will be further discussed in Section 2). Such detuned light therefore mainly acts as a potential well for the atom, hence being a trap. The volume of this trap is so small that two atoms cannot be at the same time in the trap (due to light-assisted collisions between the atoms). The typical depth of such tweezers is $\sim 1\,\mathrm{mK}$, which is enough to trap atoms that have a temperature of $\sim 100\,\mu\mathrm{K}$.

Exercise 1. Compute the speed of a Cesium 133 atom in a 300K environment. Considering using a laser tuned to be on resonance with the D_2 line, compute the typical

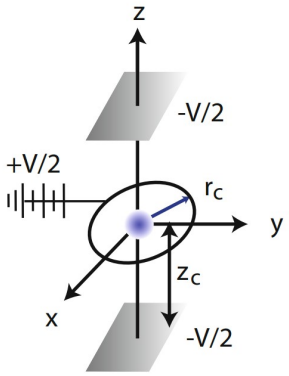

Figure 1: Quadrupole trap geometry

number of emission-absorption cycles this atom must undergo to reach a temperature of $100\,\mu$K. Assuming that Cesium atoms travel along a well defined direction, compute the typical distance which is required to cool and trap a Cesium atom. Deduce the typical size of a vacuum system used in a neutral atom quantum computer.

A challenge for the neutral atom platform is the fact that the trap depth is less than the energy of untrapped background atoms and molecules (1 mK trap depth against particles at 300 K). Collisions with hot, untrapped particles remove trapped atoms. At atmospheric pressure, the collision rate would be so high that atoms would remain trapped for durations well below 1 ns, which is way too small for performing computation. We thus put the atoms into a vaccuum chamber, with a typical vacuum of $\sim 10^{-14}$ bar. In such apparatuses, the typical collision rate is of the order of one event every 100 seconds.

1.2 Trapping ions using Paul traps

Although optical traps are possible for ions, by far the most widely used approach is an electromagnetic trap based on radio and microwave frequency fields. Consider a positively charged ion. We would like to design a trapping potential that stably confines the ion at a fixed position in space. Let $\varphi(r)$ be a static trapping potential so the energy of the ion is $U(r) = q\varphi(r)$ with q the charge. The local electric field is $E = -\nabla\varphi$, and in free space $\nabla \cdot E = -\nabla^2\varphi = 0$. In order to have a stable trap we require that φ has a local maximum or minimum which implies that $E = -\nabla\varphi$ must be either negative or positive along all lines originating at the extremum. This is not possible since $\nabla \cdot E = 0$ so there can be no local maximum or minimum of φ, only a saddle point. A saddle point can be generated in a quadrupole configuration (Figure 1) performed in the following way:

- Along the z direction of space one dimensional electrodes are placed at a distance z_c from the trap center. The potnetial of these electrodes is set to be $-V/2$
- Along the x and y directions of space, an electrode with a circular shape is placed, at a distance r_c from the trap center, and with a potential $+V/2$.

Choosing $r_c = \sqrt{2} z_c$, the obtained potential is

$$U(x, y, z) = \frac{qV}{4z_c^2}(x^2 + y^2 - 2z^2) \tag{1}$$

For $V > 0$ the potential has a quadratic maximum at $z = 0$ and minimum at $x = y = 0$.

Designed that way, the trap is metastable. To achieve stability it is necessary to add additional fields. The *Paul trap* provides a solution that confines the ions to well defined spatial positions. To do so we apply a potential $V(t) = V_0 \cos(\omega_{\text{rf}} t)$ with typical values $\omega_{\text{rf}} \sim 10 - 100$ MHz. The potential changes sign at frequency ω_{rf} which stabilizes the ion. The ion's motion along the z direction is given by:

$$\frac{d^2 z}{d\tau^2} = 2\tilde{q}_z \cos(2\tau) z \tag{2}$$

with $\tau = \omega_{\text{rf}} t/2$ a dimensionless time and $\tilde{q}_z = 2qV_0/(mz_c^2\omega_{\text{rf}}^2)$ and m is the mass. A similar equation describes the x and y motions with $\tilde{q}_x = \tilde{q}_y = -\tilde{q}_z/2$. Due to the oscillating electric field, the ion's position also oscillates. Critically, this oscillation is centered at the center of the Paul trap: the ion is stably trapped into a defined region of space. This is a Mathieu equation and it can be shown that the motion is bounded for particular value ranges of $\tilde{q}_z$. The primary stability region is $0 \leq \tilde{q}_z \leq 0.908$ which corresponds to $\omega_{\text{rf}} \geq 1.48(qV_0/(mz_c^2)^{1/2}$. This stability condition can be understood qualitatively from the requirement that the potential change sign before the accelerated ion reaches an electrode.

Exercise 2. Assuming a Be^+ ion in a Paul trap as described above with $V_0 = 100$ V and $z_c = 1$ mm, compute the minimal value of ω_{rf} which satisfies the condition on the stability region described above.

Of particular importance is the fact that the effective potential is very deep (in the range $\sim 1000 - 10000$K). If the ion were to move a tenth of the distance to the z electrode or $z/10$ the corresponding potential depth would be ~ 1000 K which is significantly larger than the energy of untrapped atoms or molecules in a room temperature vacuum apparatus. This implies that ions in a Paul trap are stable in the presence of background collisions. However, chemical reactions with untrapped particles can happen which lead to ion losses. For this reason, the ions are placed in a vaccuum chamber, with residual pressures similar to the one described in the neutral atom platform. In such environment, it has been demonstrated that ions lifetime can reach typically one month.

In this section we described the trapping of a single ion. The actual electrode geometry that is used in practice for ion traps is quite different than discussed in order to scale to many ions, but the principles remain the same.

The overall scheme to trap ions is the following: a vapor of the desired atomic species is placed inside a vacuum chamber. At the position of the Paul trap, lasers are used to ionize the atom to create the desired ion. Once this process is performed, the ion is sensitive to the Paul trap and gets trapped. Laser cooling techniques are then used on the ion in order to reduce its temperature in the Paul trap and pin it at its bottom.

1.3 Electronic qubit and center of mass motion

Following what we've discussed, the overall architecture of an atomic qubit quantum computer contains three main parts: (1) a vacuum chamber in which the atoms are confined, (2) lasers which manipulate the atoms, and (3) electronics which control the lasers.

We saw that in both platforms, the atomic qubit is trapped. In practice, it is the center of mass of the atom which is trapped, while the qubit deals with the electrons that gravitate around the center of mass of the atom. Therefore, both the qubit and the center of mass should be considered when performing quantum computations, when necessary. In the following, we will consider a qubit encoded in electronic states $|0\rangle, |1\rangle$, and a thermal state for the center of mass atomic motion. We will assume the traps to be harmonic oscillators (here one dimensional to simplify), meaning that the energy levels of the center of mass are given by $E(n) = h\omega(1/2+n)$, with ω the vibrational frequency. We will also assume that the dynamics of the center of mass within the trap follows a Maxwell Boltzmann thermal distribution, where the probability of occupation of level n is $P_n = a\exp(-U(n)/k_BT)$, with a a normalization constant. The temperature can be expressed as $k_BT = h\omega\ln(1+1/n)$. For a qubit with state $|\psi\rangle$, the complete density operator describing the atomic state is thus

$$\rho(\psi) = |\psi\rangle\langle\psi| \otimes \sum_n P_n |n\rangle\langle n|, \tag{3}$$

where the tensorial product allows for the distinction between the electronic states and the motional states of the center of mass.

Even though the description of the qubit is the same between the two platforms, there is an important difference between them: the typical reachable trap depth. For the neutral atom platform, the typical trap depth is 1 mK, with trapping frequencies in the range of $\sim 100\,\text{kHz}$. For trapped ions, the trap depth is ~ 1000 K, and the typical trapping frequencies are in the MHz range. This difference induces that the task of cooling the center of mass in the trap is much simpler to perform in ion traps than in neutral atoms, usually leading to higher fidelities in the various quantum processes which are applied.

This subtle consideration between the electronic qubit and the trapped center of mass will play an important role in the next sections, both to compute the leading decoherence term in the neutral atom platform (Section 2.2.1), and to engineer two qubit gates in the ion platform (Section 4.2).

1.4 Choice of the atomic species

In both platforms, the ability to laser cool the atomic qubit is paramount. Quantum computers based on atomic qubits are therefore limited to the atoms that can be efficiently laser-cooled. Such atoms are usually alkali-like atoms, which only have one or two valence electrons and therefore the underlying energy levels are simple to manipulate. This means that for neutral atoms, alkali atoms are mostly used, at the exception of Ytterbium Yb : $[\text{Xe}]4f^{14}6s^2$ which has 2 valence electrons (hence harder control) but

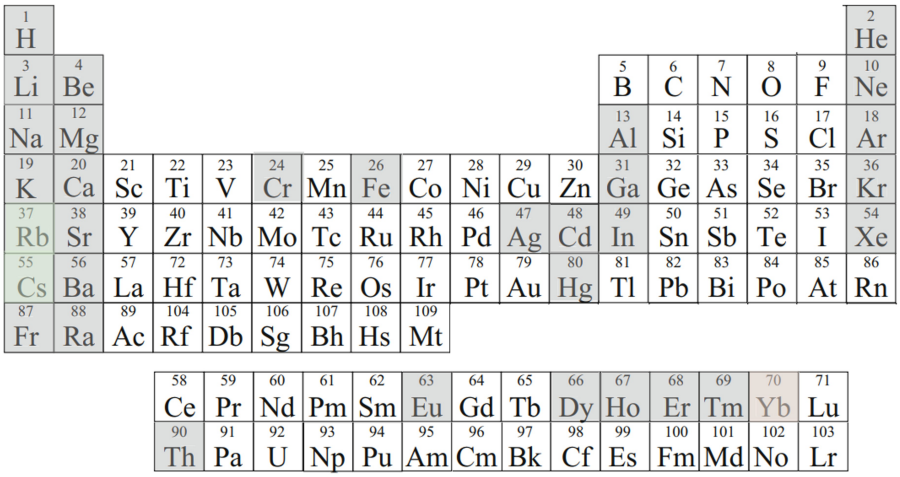

Figure 2: Shaded elements have been laser cooled and in many cases trapped in either neutral or singly ionized form. Highlighted are the leading species for neutral atom (Rb, Cs and Yb) and ions (Yb^+).

exhibits interesting properties for quantum error correction. For ions, the most commonly used species are alkaline-earth atoms with a single electron default, meaning that here also there is a single valence electron ($Yb^+ : [Xe]4f^{14}6s^1$).

A second important aspect is that the atom should be as localized as possible at the bottom of the trap in order to ease its control. For a given atom temperature, the atom's position depends on the mass of the atom: the higher it is, the more localized the atom is. This means that heavy atoms are preferred. For neutral atoms, the most common choice of atomic species are **Rubidium**, **Cesium** (heaviest alkali atoms which are stable) and **Ytterbium**. For trapped ions, the heaviest stable alkaline-like ion is $\mathbf{Yb}^+$, and is thus the common choice. In the next sections, we will discuss the case of a single valence electron (thus consider Rubidium, Cesium and Yb^+). All the reasoning would also apply to more complex electronic structures.

2 Qubit states and qubit quality

Once atoms are individually trapped, the next requirement is the ability to convert these atoms into qubits and manipulate them. As previously mentioned, the aim is to target for a qubit which has high T_1 and T_2 times. To this end, the chosen states must have long lifetime, and it is therefore natural to choose the electronic ground states as a qubit basis, as their lifetime is $\tau_{\text{gs}} \sim 10^{15}$ s. Thanks to the spin interaction between the atom's core and the valence electron, there are in most cases more than one state within the ground state manifold (for atomic species which have a non-zero nuclear spin). A subset of these ground states are then used as a qubit (see Figure 3 for Cesium). Due to the small value of the nuclear magneton these qubits have only small energy separations in modest magnetic fields. The typical energy splitting is in the range of $\sim 2\pi \times 5 - 10\,\text{GHz}$:

- For Rubidium, $\omega_{10} \simeq 2\pi \times 6.8\,\text{GHz}$

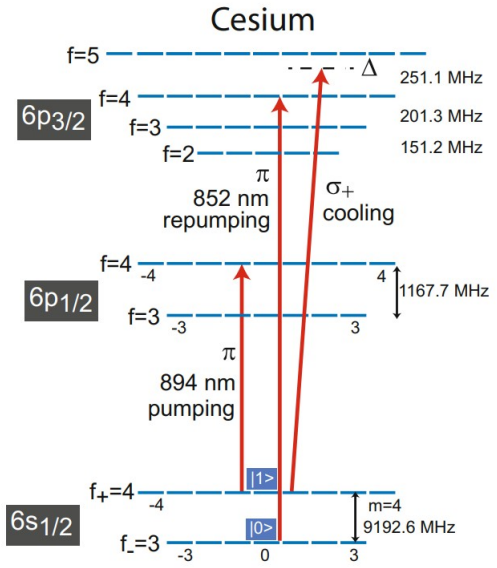

Figure 3: Structure of low lying energy levels of Cs (representative of the states for Rb, Cs and Yb^+). Cs hyperfine qubits are encoded in Zeeman sublevels of $f_+ = 4$ and $f_- = 3$. Optical transitions to the lowest lying excited states are used for cooling and state preparation.

- For Cesium, $\omega_{10} \simeq 2\pi \times 9.2\,\text{GHz}$
- For Yb^+, $\omega_{10} \simeq 2\pi \times 12.2\,\text{GHz}$

The transition frequency between the two states is thus (1) low enough such that it can be performed by applying a microwave field using extremely well controlled radio-frequency generators, and (2) large enough such that the Rotating Wave Approximation can be applied (for the typical gate speeds that are currently used). We will see in the next section that these extremely nice properties enable high single-qubit gate fidelities.

2.1 Qubit lifetime T_1

We now study the typical T_1 time that is obtained using atomic qubits. As a reminder, the T_1 quantifies the typical states lifetime of $|0\rangle$ and $|1\rangle$. Even though it is in theory possible that both states do not have the same lifetime, in practice for the atomic qubit platforms it is the case. The theoretical lifetime of the $|0\rangle$ and $|1\rangle$ states is $\tau_{\text{gs}} \sim 10^{15}$, and thus one could expect $T_1 \sim \tau_{\text{gs}} \sim 10^{15}$. However in practice, the obtained value of T_1 is lower, because these atoms are coupled to their environment, We consider two factors common to ions and neutral atoms that induce a reduction of T_1:

- Due to black-body radiations, the atomic qubits can absorb electromagnetic waves emitted from the environment and therefore undergo unwanted transitions. However, the coupling between the qubit states being very weak, the expected reduced T_1 from this effect is $T_1^{\text{BBR}} \sim 10^{-12}$ s. This shows that a cryogenic environment is not necessary for atomic qubits, in contrast to superconducting circuits which will be studied in Lecture 3.

- Even though the atomic qubits are placed in a vacuum chamber, there is a certain probability that a trapped atomic qubit collides with background residual gas. The magnitude of this factor depends on the quality of the vacuum, and is generally in the 100 s regime.

Exercise 3. Considering rubidium 87, derive the impact of black-body radiation given above ($T_1^{\mathrm{BBR}} \sim 10^{-12}$ s) at 300K using the thermal photon occupation formula of a 300K environment.

Considering these two mechanisms, the obtained T_1 time can reach hours, making it the highest value among all quantum computing platforms.

However in the case of the neutral atoms, the T_1 time is much lower, as a third mechanism contributes to reducing the T_1 time. As the atoms are trapped in optical tweezers, there is a finite probability for the atom to absorb the light from the tweezers, a phenomenon known as Raman scattering. This scattering depends on the atomic species. For alkali atoms, the Raman scattering rate Γ_R is given by:

$$\Gamma_R = \frac{\Gamma U}{3\hbar} \frac{\Delta_{\mathrm{FS}}^2}{\Delta^2}, \tag{4}$$

where Δ_{FS} and Γ are respectively the fine-structure splitting and linewidth of the first excited state, Δ is the detuning from the fine-structure center, and U the tweezers trap depth. This formula shows that, for a fixed atomic species, this phenomenon depends on: (1) the wavelength of the light (via Δ and U), and (2) the laser intensity (via U). In practice, the tweezers depth U is fixed (as a certain depth is required to efficiently trap and keep the atoms in the tweezers), and therefore the only free parameter is the trapping laser wavelength. Thankfully, $U \propto 1/\Delta$ whereas $\Gamma_R \propto 1/\Delta^2$, meaning that Γ_R can be arbitrarily decreased while keeping a trap depth of 1 mK. In typical nowadays quantum computer, the Raman scattering is in the range of seconds, and up to hundred seconds has been demonstrated.

Exercise 4. Considering rubidium 87, compute the Raman scattering rate for light at 820 nm and assuming a trap depth of 1 mK. Also compute the laser power required to trap an atom, assuming that the optical tweezers has a Gaussian profile with a radius waist of $1\,\mu$m. Perform the same computations (Raman scattering rate and required laser power) now assuming a wavelength of 850nm. What conclusion do you reach from these calculations? Can you provide an advice on the tweezers wavelength one should use to build a neutral atom quantum computer?

As a conclusion, the typical T_1 of nowadays neutral atom quantum computer is in the range $T_1 \sim 1$ s, mainly limited by Raman scattering from the optical tweezers whereas the typical T_1 time obtained in trapped ions is $T_1 \sim 10^3$ s, the difference coming from the underlying method used to trap the atomic qubit.

2.2 Qubit coherence time T_2

We now study the typical T_2 time that is obtained using atomic qubits. As a reminder of Lecture 1, the T_2 time quantifies the quality of a qubit to remain in a superposition

state of $|0\rangle$ and $|1\rangle$. Its measurement is usually performed via Ramsey interferometry, which has been studied in Lecture 1. As a reminder: starting from $|0\rangle$, a first rotation around the y axis $R_y(\pi/2) = e^{-i\pi/4\hat{Y}}$ is performed, which prepares the state $|+\rangle = (|0\rangle + |1\rangle)/\sqrt{2}$. The system then evolves for a duration t under the operator $U(t) = R_z(\delta t) = e^{-i\delta t/2\hat{Z}}$, with δ the detuning between the driving field frequency, and the qubit transition frequency (assuming the rotating wave approximation), leading to the state $(|0\rangle + e^{-i\delta t}|1\rangle)/\sqrt{2}$. A last $R_y(\pi/2)$ is performed before measuring the populations in $|0\rangle$ and $|1\rangle$. The complete unitary U_R which is performed is $U_R(t) = R_y(\pi/2)U(t)R_y(\pi/2)$, and the outcome of this experiment is $P_0(t) = \sin(\delta t/2)^2$.

The T_2 time is the typical duration after which the overlap of the evolved wavefunction $|\phi(T)\rangle$ onto $|+\rangle$ is below $1/e$. We note that the definition of T_2 can slightly vary depending on the underlying decoherence mechanisms and quantum computing platforms (as seen in Lecture 1, the overlap decay is not always exponential).

Several factors contribute to the value of T_2. First, the T_2 time is directly dependent on the T_1 time as discussed in Lecture 1, as for example an event of spontaneous emission from $|0\rangle$ or $|1\rangle$ would collapse the wavefunction, and lead to $T_2 = 2T_1$. The T_2 time is also impacted by decoherence mechanisms that suppresses the coherence between $|0\rangle$ and $|1\rangle$, which in the density matrix formalism correspond to the terms ρ_{01} and ρ_{10}. Such coherence terms are decreased when submitted to decoherence mechanisms, leading to non-pure state.

However in practice, the coherence terms are mostly impacted by unwanted phases added between the $|0\rangle$ and $|1\rangle$ states. This modifies the state and therefore reduces the T_2 time, but do not lead to *decoherence* in its mathematical definition (the state after unwanted phases variations is still a pure state). However, if the quantum computer is not aware of this (coherent) change of state, then it isn't possible to backtrack the original state, and therefore the system behaves as if it was incoherent. In practice, such "coherent" errors are largely predominant, and usually arise from fluctuations in the energy difference between the two levels of the qubit. In the Ramsey sequence described above, it means that δ follows a certain (random) distribution, and the obtained P_0 is then a damped sine (see Lecture 1) with an associated T_2 value.

For both platforms, a main factor that contributes to T_2 is static electric and magnetic field fluctuations. The electron in its ground state is largely insensitive to electric field fluctuations. We stress that it is also the case for ions: even though the center of mass of the ion is extremely sensitive to electric field (hence the trapping), the electron that gravitates around the center of mass is not, as the energy levels in the ground states are mainly coming from the spin interaction between the electron and the center of mass.

To prevent the impact of magnetic field fluctuations, the energy levels that are used for the qubit are chosen to be insensitive to magnetic field at first order. Considering these, the typical T_2 time that is achieved on the ion platform is $T_2 \sim 1 - 10\,\mathrm{s}$. We will see next that it is not the case at all for neutral atoms, as another important decoherence term appears due to the trapping potential.

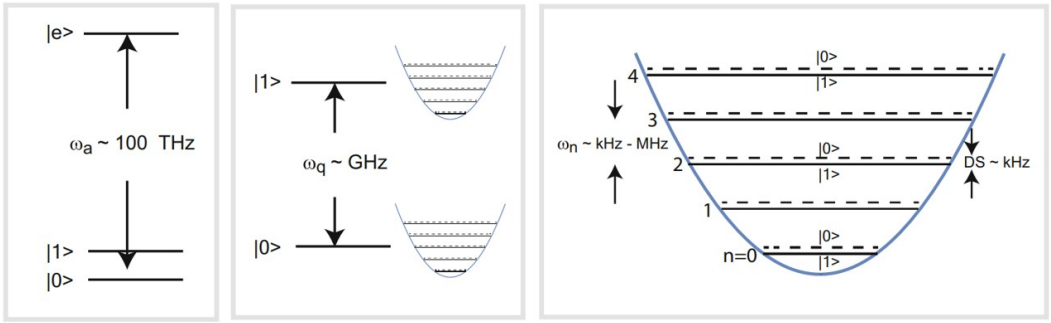

Figure 4: An electronic qubit encoded in hyperfine ground states $|0\rangle$ and $|1\rangle$ of an atom with an electronically excited state $|e\rangle$. The qubit has a GHz scale frequency ω_q and is confined in a harmonic trap with vibrational levels n separated by ω_n. Coupling between the spin and center of mass degrees of freedom results in a small spin dependent differential shift (DS) of the vibrational energies.

Exercise 5. Considering rubidium 87, compute the energy shift that is applied to the ground states due to a static electric field of 1 V/cm (compare with the situation of 0 electric field). Perform the same for a magnetic field of 1 Gauss. Out of the 8 ground states of Rubidium, find the best qubit based on these calculations.

2.2.1 Motional decoherence in neutral atoms

The variations in the energy levels due to the trapping potential have two origins: (1) fluctuations of the laser power itself, and (2) variations induced by the movement of the center of mass in the trap (also known as *motional dephasing*). As the center of mass oscillates in the trap, the light intensity that the atom feels varies in time. This varying light intensity induces variations in the energy of the atom's levels. As the two levels of the qubit do not experience the same light shift induced by the tweezers, this effect leads to decoherence. Motional decoherence provides an instructive example of undesired entanglement between the qubit and other dynamical variables, which here results in reducing the coherence time (Figure 4).

As previously discussed the T_2 time can be measured with Ramsey spectroscopy, which involves the sequence $U_R = R_y(\pi/2)U_n(t)R_y(\pi/2)$. As we now consider the impact of the center of mass movement which changes the electron's energy levels, the free evolution operator for a time t is now given by

$$U_n(t) = e^{-i(\Delta_m(n)-\delta)\hat{Z}t/2}. \tag{5}$$

Here $\delta = \omega - \omega_{10}$ is the detuning of the field driving from the qubit frequency ω_{10} (same as above), $\Delta_m(n) = \frac{1}{\hbar}[E_1(n) - E_0(n)] = (1/2 + n)(\omega_1 - \omega_0)$ is the differential light shift between the two qubit states, and ω_j are the trap frequencies when the atom is in the electronic state $|j\rangle$. We will assume R only acts on the electronic state and does not change $|n\rangle$.

The trap frequencies depend on the electronic state due to the fractional differential

light shift $E_{\rm LS} = (E_1 - E_0)/\frac{1}{2}(E_0 + E_1)$. The energy difference $\Delta E = E_1 - E_0$ scales as

$$\Delta E \sim \bar{E}(\frac{\Delta}{\Delta - \omega_q/2} - \frac{\Delta}{\Delta + \omega_q/2}) \simeq \bar{E}\frac{\omega_q}{\Delta} \tag{6}$$

with $\bar{E}$ the average trap potential and Δ the detuning of the trap light from the excited state. Using a trap depth $\bar{E} = k_B \times 1$ mK , $\omega_q \sim 2\pi \times 10$ GHz and $\Delta \sim 2\pi \times 10$ THz, we obtain $\Delta E \sim h \times 20\,$kHz.

With the assumption of $\Delta_{\rm LS} \ll 1$, which is generally the case, we can write $\omega_1 \simeq \omega_0(1 + \bar{\Delta}_{\rm LS}/2)$ so $\Delta_1(n) = (1/2 + n)\omega_0\bar{\Delta}_{\rm LS}/2$. The density matrix after a Ramsey sequence is therefore:

$$\rho(t) = U\rho(0)U^\dagger = R_{\pi/2}U_n(t)R_{\pi/2}\left(|0\rangle\langle 0| \otimes \sum_n P_n |n\rangle\langle n|\right) R^\dagger_{\pi/2}U_n(t)^\dagger R^\dagger_{\pi/2} \tag{7}$$

The probability of measuring the atom in $|1\rangle$ after time t is $P_{|1\rangle}(t) = {\rm Tr}_{\rm vib}(\langle 1|\,\rho\,|1\rangle) = \sum_n P_n |\langle 1|\, R_{\pi/2}U_n(t)R_{\pi/2}\,|0\rangle\,|^2$, where ${\rm Tr}_{\rm vib}$ denotes the trace over the motional states (as the detection is not sensitive to the ionic core motion). Evaluating the operator product we find

$$P_{|1\rangle}(t) = \frac{1}{2} + \frac{1}{2}\sum_n P_n \cos(\theta_n t) \tag{8}$$

with $\theta_n = \frac{\bar{\Delta}_{\rm LS}}{2} n\omega_0 - \delta$. When the atom is in the motional ground state $P_0 = 1$ and $P_{|1\rangle}(t) = \frac{1}{2}(1 + \cos(\delta t))$. We here recover the results of the usual Ramsey experiment.

For thermal states with many occupied vibrational modes evaluation of the above sum is inefficient. In this limit we can let $\hbar/T \to 0$, use $P_n \simeq \omega_x\omega_y\omega_z\beta^3 e^{-\beta n\omega_0}$, and approximate the sum by an integral. This semiclassical approximation leads to

$$P_{|1\rangle}(t) = \frac{1}{2} + \frac{1}{2[1 + 0.948(t/T_2^*)^2]^{3/2}}\cos(\delta t - \kappa) \tag{9}$$

with $T_2^* = \sqrt{e^{2/3} - 1}\frac{2\hbar}{k_B T\bar{\Delta}_{\rm LS}}$. For typical parameters $T = 10\,\mu$K and $\Delta_{\rm LS} = 2\pi \times 20$ kHz, one obtain $T_2^* \sim 1$ ms. This means that the coherence time is strongly limited by this effect.

Exercise 6. Find the expression of κ.

From this result, we can make a few key observations:

- As discussed in Lecture 1, not all types of noises lead to an exponential decay of Ramsey fringes contrast. Motional decoherence as detailed above is one of them.
- The coherence time T_2 is directly linked to the the introduced effective coherence time T_2^*. Its value depends on the atom temperature (for zero-temperature no decay is expected), as well as the fractional differential light shift. In the limit of an infinitely detuned trapping light, the $|0\rangle$ and $|1\rangle$ states would feel the exact same light-shift, and therefore $T_2^* \to \infty$. Another solution to cancel this decoherence mechanism is to have the same trapping potential for both states of the qubit. This situation is called *magic trapping*, and is widely used in atomic clock experiments.

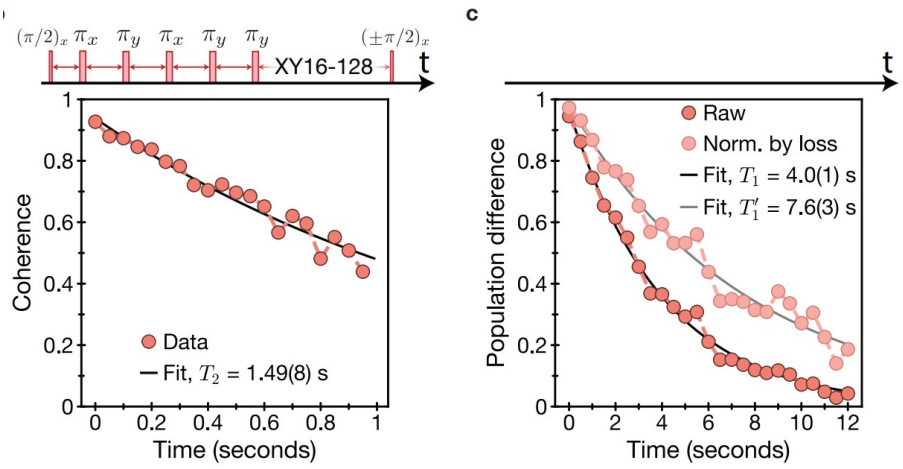

Figure 5: Experimentally measured $T_1 \simeq 4$ s and $T_2 \simeq 1.5$ s (with dynamical decoupling) on the neutral atom platform.

This motional decoherence error is inherently *coherent*, and the decoherence arises from the fact that the motional states are randomly populated. As previously discussed, if we were able to track the motional states of the atom's center of mass, we could be able to compensate this effect.

2.2.2 Canceling motional dephasing through dynamical decoupling

Another solution cancels motional dephasing: the use of *dynamical decoupling* methods. As discussed in the Lecture 1, the simplest one is the spin-echo (or Hahn) sequence. Starting from $|0\rangle$, it consists in applying between the two $\pi/2$-pulses of the Ramsey sequence a π-pulse that flips the qubit states $|0\rangle$ and $|1\rangle$. half of the sequence, after the π-pulse, leads to a rephasing of the dynamics. The implemented unitary is the following:

$$U_{\mathrm{SE}} = R_y(\pi/2)U(t)R_y(\pi)U(t)R_y(\pi/2) \tag{10}$$

where for the sake of simplicity, we will here consider the simple case $U(t) = R_z(\delta t)$. One can show that in this situation, $P_0 = 1$, whatever the values of δ and t. Such dynamical decoupling cancels motional dephasing, but also any "coherent" noise which does not vary between the beginning and the end of the sequence: assuming the evolution $R_y(\pi/2)U(t)R_y(\pi)U'(t)R_y(\pi/2)$, the echo method works if $U(t) = U'(t)$.

Exercise 7. Demonstrate that $P_0 = 1$ in the echo sequence described above.

Using such methods, the T_2 time can be extended to values as high as $\sim$ 1s. For such duration, the T_1 becomes the main contributor. As the T_1 time is dominated by an incoherent process (spontaneous emission), it cannot be dynamically decoupled.

2.3 Comparison between neutral atoms and ions

In this section, we have analyzed the leading mechanisms that explain the obtained T_1 and T_2 times. Typical values are reported in FIgure 5. We have observed that trapped

ions outperform neutral atoms on this two values, in particular due to the trapping method which is employed: as the Paul trap does not directly act on the electron's energy levels in order to trap the atom's center of mass, its impact on the qubit is negligible. This is in contrast with optical tweezers traps which directly use the valence electron in order to trap the center of mass.

From this, the conclusion could be that trapped ions are better than neutral atoms. However, an important key parameter here is the *scalability* of the platforms: realizing in practice arrays of Paul traps is a large technical challenge, whereas creating arrays of optical tweezers is a relatively simple task. We therefore have a trade-off between qubit number and qubit quality between the two platforms.

2.4 Qubit detection

We briefly mention how atomic qubits are detected. For both platforms, the adopted solution is to perform fluorescence imaging by shining resonant light which targets only one state of the qubit. The spontaneously emitted light by the atomic qubits is collected using a camera. Assuming that it is the $|1\rangle$ state that is targeted by the light, atomic qubits that emitted light are inferred to be in the $|1\rangle$ state, while atomic qubits that do not emit light are inferred to be in the $|0\rangle$ state.

3 Single qubit gates

For both platforms, single-qubit gates are implemented via microwave or optical frequency fields through Raman transitions. The gates are implemented via Rabi drive. The Hamiltonian that describes resonant Rabi driving is:

$$H = \frac{\hbar\Omega}{2}(\cos(\phi)X + \sin(\phi)Y), \tag{11}$$

where Ω is the Rabi frequency and ϕ the driving phase. In particular, $R_x(\theta)$ or $R_y(\theta)$ rotations can be engineered with the correct value of ϕ. The rotation angle is $\theta = t\Omega$ with t the gate time. Rotations about other axes in the equatorial plane can be obtained with an appropriate choice of ϕ. Phase gates are implemented by changing ϕ. As any angles θ and ϕ are accessible, it means that any single qubit rotation can be performed. These consideration highlight the importance of having a good control over the driving phase.

Exercise 8. Show on a Ramsey experiment that changing the phase of the second pulse by a quantity ϕ is equivalent to applying $R_z(\phi)$ during the Ramsey experiment.

Gates acting on qubits encoded in hyperfine states can be simply implemented using microwave fields that are resonant with the qubit frequency. When the hyperfine states are connected with the same electronic orbital the transition is of magnetic dipole character and the Rabi frequency is $\Omega = \mu B/\hbar$ where μ_B is the matrix element of the magnetic moment operator and B is the amplitude of the magnetic field. For radiation of intensity I the field amplitude is $B = \mathcal{E}/c = \sqrt{2I/(\epsilon_0 c^3)}$, where $\mathcal{E}$ is the electric

field amplitude. Typical Rabi frequencies for a few watt of microwave power driving a hyperfine transition in an alkali atoms are $\sim 10\,\mathrm{kHz}$.

All qubits in an array can be rotated in parallel by turning on a resonant microwave field. Since the microwave wavelength is much longer than a typical atomic array size all qubits are addressed. Site selective addressing can be achieved with a combination of microwaves and a focused optical beam that Stark shifts selected sites. Site specific x or y rotations are then obtained using the identity:

$$R_x(\theta) = \bar{R}_y(\pi/2) R_z(\theta) \bar{R}_y(-\pi/2) \tag{12}$$

Here $\bar{R}_x$ and $\bar{R}_y$ are global rotations which cancel at those sites that do not receive the local R_z rotation.

Exercise 9. Show how to implement a local $R_y(\theta)$ rotation using global $\bar{R}_x$ rotations and local R_z rotations.

Even though microwaves are the simplest solution, they lack two features:

- Their low Rabi frequency (in the 10 kHz range) means that gate operations are slow (typically 100 μs), meaning that the quantum computer will be slow.
- The lack of direct qubit adressability induces a loss of fidelity in the operations, and increases the complexity of computations.

Faster Rabi frequencies can be achieved using optical transitions, using a two-photon stimulated Raman transition via an excited state. In general the selected excited state is the first excited state ($5P_{1/2}$ for Rubidium). This involves a light field consisting of two optical frequencies with the difference equal to the qubit frequency. If the one-photon Rabi frequencies are Ω_1, Ω_2 with respect to an intermediate state that is detuned by Δ then the two-photon Rabi frequency is $\Omega_1\Omega_2/(2\Delta)$. With the optical Raman approach Rabi rates of several MHz can be readily achieved, meaning that gate execution is performed in duration below 1 μs. There is a decoherence cost associated with this approach since photons are scattered from the intermediate level. It can be shown that the probability of photon scattering during a π pulse is $P_{\mathrm{scat}} \sim \gamma/|\Delta|$ where γ is the radiative decay rate of the intermediate state.

Exercise 10. Assuming that $\Omega_1 = \Omega_2$, demonstrate the formula giving the amount of scattering during a π pulse.

The typical single-qubit gates fidelities on current neutral atom platforms is $F_{1Q} \simeq 99.99\%$, and reaches $F_{1Q} \simeq 99.999\%$ in trapped ions. These values are mainly limited by scattering, as well as power and frequency fluctuations in the drive which lead to coherent errors (the performed gate is not exactly the intended one).

Exercise 11. Assuming Rubidium 87, compute the typical one-photon Rabi frequency using a laser on resonance on the D_1 line (795 nm) using a laser with a power of 1 mW with a Gaussian profile and a radius waist of 100 μm. Assuming a second laser identical

to the first one and set to perform the Raman transition, and a measured $T_1 = 10\,\text{ms}$ for both qubit states, what is the optimal value of Δ which maximizes the single qubit gate fidelity, and what is the expected fidelity?

4 Two-qubit gates

Interactions between qubits are needed to implement two-qubit gates. In both ions and neutral atoms, the chosen states for the qubit encoding interact very weakly with their environment (hence having high T_1 and T_2 times), and hence with nearby atomic qubits. The two platforms uses very different methods in order to engineer interactions: neutral atoms use the natural dipole-dipole interaction between atoms to engineer two qubit gates, whereas tapped ions uses the motion of the center of mass. We successively describe these two.

4.1 Engineering two qubit gates with neutral atoms

4.1.1 Dipole-dipole interaction and Rydberg states

We use the dipole-dipole interaction between atoms to engineer two qubit gates. Considering two dipoles separated by a distance r, the general formula of the dipole-dipole interaction is given by:

$$V_{dd} = \frac{1}{4\pi\epsilon_0}\frac{\vec{d_1}\cdot\vec{d_2} - 3(\vec{d_1}\cdot\vec{r})(\vec{d_2}\cdot\vec{r})}{r^3} \tag{13}$$

where $\vec{d_1}$ and $\vec{d_2}$ are the dipole moments of the two considered dipoles. The dipole dipole interaction typically scales as $V_{dd} \sim d^2/r^3$. Here, d is linked to the size of the dipole, and for atoms the dipole size is typically given by the spatial extent of the electron's wavefunction $d \simeq a_0 n^2$ where a_0 is the Bohr radius and n the principal quantum number.

As electronic levels have a definite parity, they do not exhibit a permanent dipole moment ($\langle\vec{d}\rangle = 0$). Therefore, the dipole-dipole interaction between two qubits in the state $|0\rangle \otimes |0\rangle = |00\rangle$ is zero:

$$\langle 00|\, V_{dd}\, |00\rangle = 0 \tag{14}$$

However, the dipole-dipole interaction is non zero between opposite parity states. Considering an energy level $|ab\rangle$ with opposite parity as $|00\rangle$, then $\langle ab|\, V_{dd}\, |00\rangle \neq 0$. This coupling to nearby states induces an *energy shift* V_{VdW}^{00} of the $|00\rangle$ state. Its value can be obtained via second order perturbation theory:

$$V_{VdW}^{00} = \sum_{a_i,b_i} \frac{|\,\langle a_i b_i|\, V_{dd}\, |00\rangle\,|^2}{E_{a_i,b_i} - E_{00}} \tag{15}$$

where the sum runs over all existing states a_i, b_i with energy E_{a_i,b_i}, and E_{00} is the energy of the $|00\rangle$ state. In general considering two atoms, this energy shift scales as $V_{VdW} \sim V_{dd}^2/\Delta \sim d^4/(\Delta r^6)$, where here Δ is the typical energy difference between

states. We observe that this energy shift takes the form of a Van der Waals interaction: $V_{VdW} \sim C_6/r^6$, with $C_6 \sim d^4/\Delta$.

We can now compute the typical energy shift between two atoms in their ground state at a distance $r = 5\,\mu$m, a typical distance between two optical tweezers. In this situation, $C_6/h \sim 10^{-7}\,\text{Hz}.\mu\text{m}^-6$, and thus $V_{VdW}/h \sim 2\pi \times 10^{-11}$ Hz. This means that the interaction is fully negligible on atoms that are in their ground state.

In order to enhance this interaction, atoms are excited to energy levels with a high principal quantum number n. The scaling of the van der Waals interaction with n is $U_{\text{VdW}} \propto n^{11}$. Now assuming $n = 75$, we obtain $C_6/h \sim 10^3\,\text{GHz}.\mu\text{m}^6$, and $U_{\text{VdW}}/h \simeq 64$ MHz. The interaction is now many orders of magnitudes stronger.

Exercise 12. Assuming an energy level repartition following the hydrogen structure, find the scaling $U_{\text{VdW}} \propto n^{11}$.

In practice, only the $|1\rangle$ state is connected to $|r\rangle$, usually using a Raman transition with a Rabi frequency Ω_r. We are here defining a novel qubit in our system, which is constituted of the states $|1\rangle$ and $|r\rangle$. Assuming a single atom, the Hamiltonian H^1_{ryd} that governs the dynamics of the system is exactly the same as for single qubit gates (simple Rabi driving):

$$H^1_{\text{ryd}} = \frac{\hbar\Omega_r}{2}(\cos(\phi_r)X + \sin(\phi_r)Y), \tag{16}$$

with ϕ_r the phase of the drive.

Now considering the case where two atoms are separated by $r = 5\,\mu$m, the relevant Hamiltonian which acts on both atoms is:

$$H^2_{\text{ryd}} = \frac{\hbar\Omega_r}{2}(\cos(\phi_r)X_1 + \sin(\phi_r)Y_1) + \frac{\hbar\Omega_r}{2}(\cos(\phi_r)X_2 + \sin(\phi_r)Y_2) + \frac{C_6}{r^6}\,|rr\rangle\langle rr| \tag{17}$$

where X_i and Y_i are the usual X and Y operators acting on atom i. We here find the van der Waals interaction term, which shifts in energy the $|rr\rangle$ level by a quantity $\frac{C_6}{r^6}$.

In typical neutral atom quantum computer, $\Omega_r \sim 2\pi \times 5$ MHz, and $U_{\text{VdW}}/h \sim 100$ MHz. We are thus in a regime for which $\Omega_r/(2\pi) \ll U_{\text{VdW}}/h$. In practice, this means that $|rr\rangle$ is so much shifted in energy by the Van der Waals interaction that the system cannot couple to this state, a phenomenon known as *Rydberg blockade*, which means that only one of the atom can go in the $|r\rangle$ state. However, as this process happens in an indistinguishable fashion between the two atoms, both atoms reach the Rydberg state, and the system thus couples to the state *entangled state* $|W\rangle = (|1r\rangle + |r1\rangle)/\sqrt{2}$: the Rydberg blockade mechanism leads to *entanglement generation*. Importantly, the coupling strength to this state is different than in the single atom case: the coupling strength between $|00\rangle$ and $|W\rangle$ is $\sqrt{2}\Omega_r$, whereas it is Ω_r between $|0\rangle$ and $|1\rangle$. This difference in coupling strength is the main feature which enables the implementation of two-qubit gates.

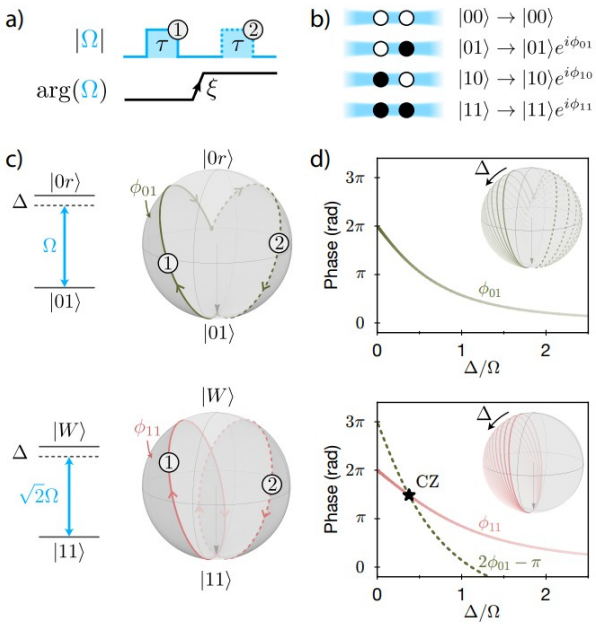

Figure 6: Levine-Pichler (LP) gate protocol. a) Pulse sequence. b) Output states of the gate protocol. c) Bloch sphere representation of the system evolution in the situation $|01\rangle$ and $|10\rangle$. The dynamics of the $|01\rangle$ and $|11\rangle$ states can be understood in terms of two-level systems with the same detuning Δ but different effective Rabi frequencies. The pulse length τ is chosen such that the $|11\rangle$ system undergoes a complete detuned Rabi cycle during the first pulse, while the $|01\rangle$ system undergoes an incomplete oscillation. The laser phase ξ is chosen such that the second pulse drives around a different axis to close the trajectory for the $|01\rangle$ system, while driving a second complete cycle for the $|11\rangle$ system. d) The dynamical phases ϕ_{01} and ϕ_{11} are determined by the shaded area enclosed by the Bloch sphere trajectory and vary from 2π to 0 as a function of Δ, corresponding to increasingly shallow trajectories. Insets show family of trajectories for different detunings. Choosing $\Delta \simeq 0.377\Omega$ realizes the CZ gate.

Exercise 13. Demonstrate that in the regime $\Omega_r/(2\pi) \ll U_{\mathrm{VdW}}/h$, the two atom Hamiltonian applied to $|00\rangle$ has a coupling strength of $\sqrt{2}\Omega_r$ to the $|W\rangle$ state.

4.1.2 Two qubit gate engineering via the Levine-Pichler protocol

We implement a CZ gate using the Rydberg blockade mechanism via the Levine-Pichler gate protocol (Figure 6). We remind the expression of this gate:

$$U_{\mathrm{CZ}} = \begin{pmatrix} 1 & 0 & 0 & 0 \\ 0 & 1 & 0 & 0 \\ 0 & 0 & 1 & 0 \\ 0 & 0 & 0 & -1 \end{pmatrix} \tag{18}$$

The gate protocol is as follows:

- A first pulse coupling $|1\rangle$ to $|r\rangle$ of duration τ, with a detuning Δ from the transition, is applied
- A phase change in the driving field of value ξ is applied to the driving field
- A second pulse, identical to the first one, is applied.

We call the unitary applied by this protocol $\mathcal{U}$. Each pulse changes the state of the atoms according to the unitary $U(\tau) = e^{-iH\tau}$. As previously discussed, the phase change can be seen as a rotation $R_z(\xi)$. Therefore, $\mathcal{U} = U(\tau)R_z(\phi)U(\tau)$. The evolutions are here performed with a detuning from the transition. Form the generalized Rabi formula, one gets the effective Rabi frequency: $\Omega_{\text{eff}} = \sqrt{\Omega^2 + \Delta^2}$ (in the case where $\Delta = 0$, we recover the usual Rabi frequency Ω).

In order to show that this protocol implements a gate close to a CZ gate, we will check the output state of the gate protocol considering the 4 input states: $|00\rangle$, $|01\rangle$, $|10\rangle$ and $|11\rangle$.

Input state $|00\rangle$: The state is not connected to the Rydberg states, and therefore nothing happens. The output state is $|00\rangle$, as expected for the CZ gate.

Input state $|11\rangle$: We choose the length of each pulse τ such that a system prepared in $|11\rangle$ undergoes a complete, detuned Rabi oscillation and returns to the state $|11\rangle$ already after the first single pulse. This means that:

$$\tau = 2\pi/\Omega_{\text{eff}} = 2\pi/\sqrt{\Delta^2 + (\sqrt{2}\Omega)^2} \tag{19}$$

As we are in the blockaded regime, the driving strength is given by $\sqrt{2}\Omega$. This means that after one pulse, the system is in the state $U|11\rangle = e^{-iH\tau}|11\rangle = e^{i2\pi\Delta/\sqrt{\Delta^2+2\Omega^2}}|11\rangle$. The phase change $R_z(\phi)$ does not impact the system, as $|00\rangle$ is in an eigenstate of $R_z(\phi)$, and therefore there isn't any dynamical phase accumulation. The second pulse also leads to a complete, detuned Rabi cycle about a different axis (due to the change in phase), but results in the same accumulated phase. At the end of the gate protocol, the total evolution leads to $\mathcal{U}|11\rangle = e^{i\phi_2}|11\rangle$ with

$$\phi_2 = 2\pi \times 2\Delta/\sqrt{\Delta^2 + 2\Omega^2}. \tag{20}$$

Input states $|10\rangle$ and $|01\rangle$: Since one of the atoms is in $|0\rangle$, the Rydberg blockade phenomenon does not take place, and the system evolves following H^1_{ryd} (with the addition of a detuning term). The dynamics is thus the same for $|10\rangle$ and $|01\rangle$, and we thus treat them together and only consider $|01\rangle$ in the following. Due to the mismatch between the effective Rabi frequencies between the blockaded regime and the single atom regime, the $|10\rangle$ state does not return to itself after the time $|\tau\rangle$ but a superposition state is created: $U|10\rangle = \cos(\alpha)|10\rangle + \sin(\beta)e^{i\gamma}|r0\rangle$. α, β and γ are determined by the choice of Ω, Δ and τ. Crucially, by a proper choice of ξ one can always guarantee that the system returns to the state $|01\rangle$ after the second pulse. With this choice of the phase

we thus have $U|10\rangle = e^{-i\phi_1}|10\rangle$.The acquired dynamical phase is a function of Δ/Ω, $\tau\omega$ and ξ. Since we fixed τ in equation (19), and ξ such that $U|10\rangle = e^{-i\phi_1}|10\rangle$, ϕ_1 is solely determined by the dimensionless quantity Δ/Ω. Note that also ϕ_2 is only a function of Δ/Ω. However, the functional dependence is different, and by setting $\Delta/\Omega \simeq 0.377$, we obtain $e^{i\phi_2} = e^{i(2\phi_1+\pi)}$.

By performing this protocol, we obtain:

$$\mathcal{U} = \begin{pmatrix} 1 & 0 & 0 & 0 \\ 0 & e^{i\phi_1} & 0 & 0 \\ 0 & 0 & e^{i\phi_1} & 0 \\ 0 & 0 & 0 & e^{i(2\phi_1+\pi)} \end{pmatrix} \tag{21}$$

which is not equal to U_{CZ}. By applying an additional phase gate $R_z(-\phi_1)$, one obtains U_{CZ}.

The exact protocol which is currently used on neutral atom quantum computer is slightly different than this one, but relies on the exact same underlying ideas. Using such protocol, CZ gates fidelities $F_{\text{CZ}} > 99.5\%$ has been demonstrated. The fidelity is impacted by various factors:

- Contrarily to ground states, the Rydberg states have a relatively short lifetime, typically $\sim 100\,\mu$s. For a typical gate duration $2\tau \simeq 400$ ns, we obtain a fidelity $F_{\text{CZ}} \sim 99.6\%$ due to the Rydberg state lifetime.
- Rydberg states are very sensitive to their environment: any magnetic field or electric field fluctuation will impact their energy level, which will cause variations in Δ. This will both impact the accumulated phase (inducing that the performed operation is not a CZ gate), and the ability for the pulses to bring the system back into the ground state qubit basis (a part of the wavefunction will remain in the Rydberg states).
- The ground-Rydberg transition frequency is $\sim$ 1000 THz, meaning that highly energetic lasers are required to perform the CZ gates. In practice, any intensity or frequency noise on these lasers will impact the gate fidelity.

4.2 Engineering two qubit gates with ions

Two-qubit gates with ions are qualitatively different than with neutral atoms. Here, the underlying mechanism enabling the generation of entanglement is the manipulation of the center of mass motion. Due to the large oscillation frequencies in trapped ions (a few MHz), it is possible to control the coupling between the qubit degrees of freedom and the center of mass motional state.

4.2.1 Coupling electronic and motional degrees of freedom

A π pulse between the qubit states can leave the motional state unchanged, remove one or more quanta of motional excitation, or add one or more quanta of motional excitation. These are referred to as carrier, red-sideband, and blue-sideband transitions

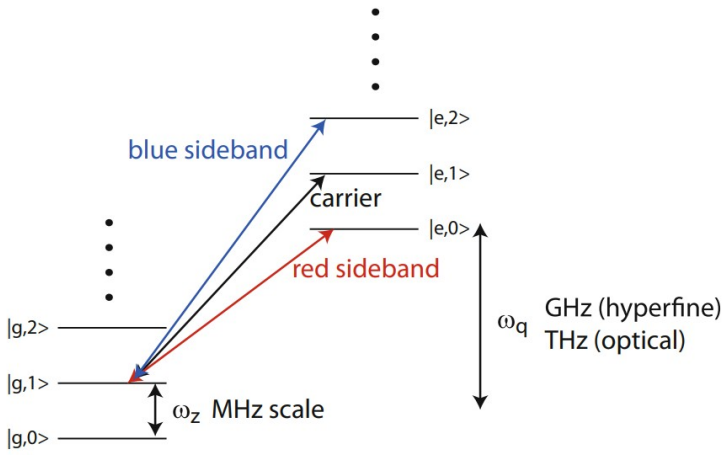

Figure 7: Electronic and motional energy levels of a trapped ion.

respectively. The quantum state of an ion $|0\rangle \otimes |n\rangle = |0, n\rangle$ is specified with two variables, the qubit state $|0\rangle$ or $|1\rangle$ and the number of motional quanta n. Unfortunately, considering the motional states $n = 0$ and $n = 1$, a confusion might arise with the qubit states $|0\rangle$ and $|1\rangle$. To avoid such confusion, the qubit states will now be referred as $|g\rangle$ and $|e\rangle$. Here for the sake of simplicity, we will assume a single trapping dimension with trapping frequency ω_z.

Physically speaking (figure 7), a field at frequency ω_q which is resonant with the qubit level spacing drives a *carrier* transition $|g, n\rangle \leftrightarrow |e, n\rangle$. A field at frequency $\omega_r = \omega_q - \omega_z$ drives a *red-sideband* transition $|g, n\rangle \leftrightarrow |e, n-1\rangle$ and a field at frequency $\omega_b = \omega_q + \omega_z$ drives a *blue-sideband* transition $|g, n\rangle \leftrightarrow |e, n+1\rangle$.

We now describe this process via Hamiltonian description. The Hamiltonian of such system can be written as $H = H_0 + H_{\text{int}}$, where H_0 accounts for the motion and qubit terms, and H_{int} for the action of the laser light onto the ion. H_0 writes as:

$$H_0 = \hbar\omega_z(1/2 + a^\dagger a) + \frac{\hbar\omega_q}{2}Z \tag{22}$$

where the first term describing the motional states energies, a and $a^\dagger$ being the the annihilation and creation operators, and the second term describes the qubit energy. For simplicity, we will drop the constant offset from this Hamiltonian. The interaction Hamiltonian can be written as:

$$H_{\text{int}} = -i\frac{\hbar\Omega}{2}e^{-i\omega t}e^{i\eta(a+a^\dagger)}e^{-i\phi}\sigma_+ + \text{h.c.} \tag{23}$$

where Ω is the Rabi frequency, ω is the field frequency, ϕ is the phase of the driving field at the ion location, and $\sigma_+ = |e\rangle\langle g|$ is the atomic raising operator. The part of this Hamiltonian that couples to the ion center of mass is $e^{i\eta(a+a^\dagger)}$. The parameter

$$\eta = \frac{2\pi}{\lambda}\sqrt{\frac{\hbar}{2m\omega_z}} \tag{24}$$

with λ the transition wavelength, is known as the Lamb-Dicke parameter. It quantifies the extent of the atomic wavefunction ($\sqrt{\frac{\hbar}{2m\omega_z}}$) relative to the wavelength of the transition, and therefore the quality that has the light to perform sideband transitions. In usual ion trap quantum computers, $\eta \sim 0.1$ and we will therefore assume next that $\eta \ll 1$.

Exercise 14. Assuming Yb^+, a laser at 355 nm and $\omega_z = 2\pi \times 5$ MHz, compute the typical Lamb-Dicke parameter value.

We perfom a first order expansion of $e^{i\eta(a+a^\dagger)} = 1 + i\eta a + i\eta a^\dagger$ and obtain:

$$H_{\text{int}} = -i\frac{\hbar\Omega}{2}e^{-i\omega t}e^{-i\phi}\sigma_+(1 + i\eta a + i\eta a^\dagger) + i\frac{\hbar\Omega^*}{2}e^{i\omega t}e^{i\phi}\sigma_-(1 - i\eta a - i\eta a^\dagger) \tag{25}$$

This Hamiltonian can be decomposed into parts corresponding to different motional state changes as $H_{\text{int}} = H_{\text{int,0}} + H_{\text{int,1}} + H_{\text{int,-1}}$ with:

$$H_{\text{int,0}} = -i\frac{\hbar}{2}(\Omega e^{i(\omega t+\phi)}\sigma_+ - \Omega^* e^{i(\omega t+\phi)}\sigma_-) \tag{26}$$

$$H_{\text{int,1}} = \frac{\hbar\eta}{2}(\Omega e^{i(\omega t+\phi)}a^\dagger\sigma_+ - \Omega^* e^{i(\omega t+\phi)}a\sigma_-) \tag{27}$$

$$H_{\text{int,-1}} = \frac{\hbar\eta}{2}(\Omega e^{i(\omega t+\phi)}a\sigma_+ - \Omega^* e^{i(\omega t+\phi)}a^\dagger\sigma_-) \tag{28}$$

The three terms correspond to carrier, blue-sideband, and red-sideband transitions introduced before. Note that the carrier transition has Rabi frequency Ω whereas the sideband transitions have Rabi frequency $\eta\Omega$ which for small η is much slower. A small Lamb-Dicke parameter not only facilitates separation of the interaction into resolved carrier and sideband transitions which is important for gate operations, but also enables cooling of the ion to its motional ground state: the η reduction of coupling to sidebands does not only apply to laser driving, but also to spontaneous emission.

Suppose we start with an ion in $|g, n\rangle$ and we drive a π pulse on the red sideband to $|e, n-1\rangle$. The ion will then spontaneously decay back to g while emitting a photon. Provided $\eta \ll 1$ the motional state cannot change so the ion decays to $|g, n-1\rangle$. Repeating this process n times the ion will end up in $|g, 0\rangle$ from which there is no red-sideband transition. This process is known as *sideband cooling*, and is used in ions quantum computers to reduce the ion temperature. This technique is also used in neutral atoms quantum computers (although more challenging to perform due to the trapping frequencies being much smaller in optical tweezers).

4.2.2 Engineering two qubit gates using the Mølmer-Sørensen (MS) gate

The gate protocol is as follows. Two ions are simultaneously illuminated by a bichromatic field with frequencies ω_+, ω_-. We choose $\omega_\pm = \omega_c \pm \delta$, ω_c is the carrier frequency, and $\eta\Omega \ll \omega_z - \delta$. As is seen in the figure 8, there are four ways in which the two ions can absorb two photons and conserve energy to make the transition $|gg, n\rangle \to |ee, n\rangle$. The

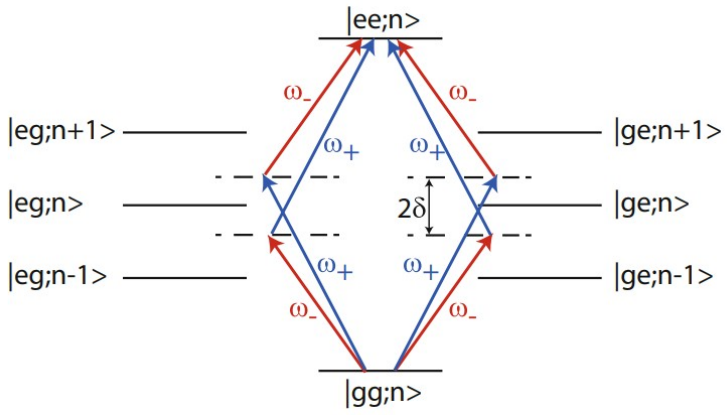

Figure 8: The MS gate uses a bichromatic laser field with frequencies ω_+, ω_- to couple ions from the $|gg\rangle$ to the $|ee\rangle$ state with one-photon carrier detuning δ.

effective Rabi rate allowing for all energy conserving paths is found from second-order perturbation theory to be

$$\tilde{\Omega} = 2\sum_{|j\rangle} \frac{\langle ee,n| H_{\text{int}} |j\rangle \langle j| H_{\text{int}} |gg,n\rangle}{U_j - U_{gg,n} + \hbar\omega_{\pm}} \tag{29}$$

with $|j\rangle = |eg, n \pm 1\rangle, |ge, n \pm 1\rangle$. Summing over the intermediate states we find the remarkable result:

$$\tilde{\Omega} = -\frac{(\eta\Omega)^2}{\omega_z - \delta} \tag{30}$$

The coupling rate is independent of the motional excitation n so Rabi pulses can be accurately applied without knowing n. Due to the η factor, the effective Rabi frequency is much smaller than Ω, which is inherent to the gate protocol as the condition $\eta\Omega \ll \omega_z - \delta$ is required for the gate protocol to function. The typical gate duration are in the range of $\sim 30\,\mu$s.

To prepare an entangled state apply ω_+ and ω_- for a time t such that $\tilde{\Omega}t = \pi/2$ which gives the transformation:

$$|gg,n\rangle \rightarrow \frac{|gg,n\rangle + i\,|ee,n\rangle}{\sqrt{2}} \tag{31}$$

We obtain a Bell state that is decoupled from the motional state, and we have thus generated *entanglement* thanks to this protocol.

The MS gate operation U_{MS} can be described as $U_{\text{MS}} = e^{-i\pi/4 Y_1 Y_2} = R_{YY}(\pi/2)$. Its expression in the computational basis is:

$$U_{\text{MS}} = \frac{1}{\sqrt{2}} \begin{pmatrix} 1 & 0 & 0 & i \\ 0 & 1 & -i & 0 \\ 0 & -i & 1 & 0 \\ i & 0 & 0 & 1 \end{pmatrix} \tag{32}$$

This gate protocol has been demonstrated to have fidelities $F_{\mathrm{MS}} > 99.9\%$. The typical gate duration is This fidelity is limited by several factors:

- Motional heating during the gate protocol. If the motional state abruptly changes during the gate execution, entanglement between the electronic state and the motional state will still be present at the end of the protocol.
- As for the neutral atom case, the gate protocol relies on lasers which have intensity and frequency fluctuations, leading to infidelities.
- The driving field is based on a Raman transition. As discussed for single-qubit gates, there is an error associated to spontaneous emission for the intermediate state used to perform the Raman process.

4.3 Universal gate set using a single two-qubit gate

For both neutral and ions platform, we have shown that one type of two-qubit gate can be implemented. Combined with the capabilities of the platform to perform any type of single qubit gate, these capabilities are enough to perform any type of gate.

Exercise 15. Assuming the neutral atom platform capabilities in terms of single- and two-qubit gates, describe a circuit which allows to implement a CNOT gate. Describe a circuit that allows to implement a Toffoli gate (described in Lecture 1).

Exercise 16. Same exercise but now considering the trapped ion platform.

5 Conclusion: performances study

With respect to other platforms (described in the next Lectures), atomic qubits exhibit extremely large T_1 and T_2 values, in the order of seconds. The gate fidelities (99.99% for single qubit gate and $> 99.5\%$ for two qubit gates) are at the level of the other platforms. The scaling perspective in qubits number of neutral atoms are pretty unique among all platforms. However, atomic qubits face various challenges.

First, the typical gate duration in atomic qubit, and in general the speed at which atomic qubits can be handled, is much longer than other platforms. We've seen that two qubit gates for ion traps take $\sim 30\,\mu$s, to be compared with $\sim 100\,$ns on other platforms. Qubit trapping, cooling, detection and manipulation in general is slow. Second, for the ion trap platform, scaling to larger qubit numbers than 100 is a delicate engineering task. Third, for neutral atom, the fact that the atoms are confined into very shallow traps and that many different techniques must be used to perform computation imposes a rigorous control over many parameters. Making all these techniques work at the same time imposes long development cycles.

References

[1] Bergou, Hillery and Saffman, Quantum information processing, Theory and Implementation, Springer (2021).

[2] Harry Levine *et al.*, Parallel Implementation of High-Fidelity Multiqubit Gates with Neutral Atoms, Physical Review letters (2019).